Ion concentration polarization on paper-based microfluidic devices and its application to preconcentrate dilute sample solutions

ARTICLE *in* BIOMICROFLUIDICS · MARCH 2015

Impact Factor: 3.36 · DOI: 10.1063/1.4913366

3 AUTHORS, INCLUDING:

Ruey-Jen Yang

National Cheng Kung University

163 PUBLICATIONS **2,741** CITATIONS

Ion concentration polarization on paper-based microfluidic devices and its application to preconcentrate dilute sample solutions

Ruey-Jen Yang, Hao-Hsuan Pu, and Hsiang-Li Wang

Citation: Biomicrofluidics **9**, 014122 (2015); doi: 10.1063/1.4913366
View online: http://dx.doi.org/10.1063/1.4913366
View Table of Contents: http://scitation.aip.org/content/aip/journal/bmf/9/1?ver=pdfcov
Published by the AIP Publishing

Ion concentration polarization on paper-based microfluidic devices and its application to preconcentrate dilute sample solutions

Ruey-Jen Yang,[a] Hao-Hsuan Pu, and Hsiang-Li Wang
Department of Engineering Science, National Cheng Kung University, Tainan, Taiwan

(Received 2 February 2015; accepted 9 February 2015; published online 18 February 2015)

Microfluidic paper-based analytical devices (μPADs) are a promising solution for a wide range of point-of-care applications. The feasibility of inducing ion concentration polarization (ICP) on μPADs has thus far attracted little attention. Accordingly, this study commences by demonstrating the ICP phenomenon in a μPAD with a Nafion ion-selective membrane. We are the first to measure the current-voltage curve on a Nafion-coated μPAD in order to indicate that the ion depletion occurs and the ICP is triggered when the current reaches the limiting current. The ICP effect is then exploited to preconcentrate fluorescein on μPADs incorporating straight and convergent channels. By an optimal geometric design, it is shown that the convergent channel results in a greater preconcentration effect than the straight channel. Specifically, a 20-fold enhancement in the sample concentration is achieved after 130 s given an initial concentration of 10^{-5} M and an external potential of 50 V. By contrast, the straight channel yields only a 10-fold improvement in the concentration after 180 s. Further, the practical feasibility of the proposed convergent-channel μPAD is demonstrated using fluorescein isothiocyanate labeled bovine serum albumin. The experimental results show that a 15-fold enhancement of the initial sample concentration (10^{-5} M) is obtained after 120 s given an external potential of 50 V. © *2015 AIP Publishing LLC*. [http://dx.doi.org/10.1063/1.4913366]

I. INTRODUCTION

Lab-on-a-chip (LOC) devices, which integrate multiple analytical steps on a single platform, have found extensive use in the chemical and biological detection fields in recent years.[1,2] Compared to conventional laboratory processes which require a large working space, expensive equipment, skilled operators, and long detection times, LOCs have several major advantages, including a lower cost, smaller sample volumes, a more rapid throughput time, and a more straightforward operation. As a result, LOCs provide an attractive solution for point-of-care (POC)[2–4] applications; particularly in developing countries or resource-poor setting areas. Among the various types of LOC available, microfluidic paper-based analytical devices (μPADs), first proposed by Whitesides' group[5] in 2007, have attracted particular attention due to their low cost and ease of fabrication, which render them ideally suited to disposable POC applications.[6,7] Reviews on recent work and perspectives in the field of μPADs are given by Li *et al.*[8] and Yetisen *et al.*[9]

The detection and analysis of proteins and DNA play a key role in disease diagnosis, and makes possible the delivery of preventative treatment if conducted sufficiently early.[10–14] However, the target proteins and DNA are generally diluted in sample solutions during the early stage of a disease, and thus collecting a sufficient number of molecules or concentration for analysis purposes is problematic.[15–19] Various researchers have shown that large numbers of charged molecules can be collected by inducing an ion concentration polarization (ICP).[18–23]

[a]Author to whom correspondence should be addressed. Electronic mail: rjyang@mail.ncku.edu.tw. Tel.: +886-6-2757575 ext. 63343. Fax: +886-6-2766549.

However, the high cost of the materials and equipment used to accomplish ICP using traditional methods limits its application for POC purposes. Consequently, the feasibility for inducing ICP in low-cost μPADs has emerged as an important concern.

Fu *et al.*[24] recently developed a simple 2-D μPAD which achieved a 4-fold improvement of concentration in the sample detection. Similarly, Chiu *et al.*[15] presented a 3-D μPAD capable of achieving a 10-fold improvement in the concentration detection of transferrin protein in less than 25 min. Leung *et al.*[25] demonstrated the existence of a streaming potential in paper-based channels; thereby confirming that cellulose surfaces have a non-zero zeta potential and can thus induce electroosmotic flow (EOF) given the application of an external electric field.

In a recent study, Gong *et al.*[26] demonstrated the application of ICP on μPADs. However, the fundamental characteristics of ICP on paper-based devices are not yet fully clear. Accordingly, the present study commences by measuring the current-voltage (I-V) curve of a Nafion-coated μPAD in order to identify the three characteristic regions of the I-V response, namely, the Ohmic current region, the limiting current region, and the overlimiting current region.[27,28] The results confirm that paper-based channels have similar electrokinetic properties to those of conventional PDMS/glass channels. Moreover, it is shown that a depletion zone (i.e., a sample concentration effect) can indeed be induced on a μPAD given the use of a suitable perm-selective membrane. In a previous study by this current group,[29] it was shown that the sample concentration effect in a PDMS/glass microchip can be enhanced by utilizing a convergent microchannel. Thus, in the present study, the ICP effect is analyzed and compared in μPAD devices incorporating either a straight microchannel or a convergent channel. By an optimal geometric design, the results confirm the effectiveness of the convergent geometry in improving the concentration effect on paper-based devices. In addition, a voltage control method is proposed for mitigating the effects of sample dispersion in order to extend the period for which the maximum sample concentration can be maintained. Finally, the practicality of the proposed convergent-channel μPAD for sample concentration purposes is demonstrated using fluorescein isothiocyanate labeled bovine serum albumin (FITC-BSA) for illustration purposes.

II. MATERIALS AND METHODS

A. Fabrication

The paper-based microchips developed in the present study were fabricated using a wax printing technique.[30] Hydrophobic barriers were designed using AutoCad 2010 and were printed on paper (Whatman No. 1 chromatography paper with 18 μm in thickness) using a commercial wax printer (Xerox ColorQube 8570). The paper was then placed in a high temperature oven (VULCAN A-550) for 1 min under 150 °C; causing the wax to melt and penetrate through the full thickness of the paper. Having produced the hydrophobic barriers, 0.6 μl of Nafion (DuPont Fluoroproducts, DE-2020) was deposited on the center of the hydrophilic chamber using a pipette. The Nanfion membranes contain nano-passages and form the micro/nano interface necessary for ion concentration polarization. The Nafion penetrates through the thickness of the paper. The μPAD was then placed in the oven at a temperature of 150 °C for 30 s in order to cure the Nafion structure. Finally, the μPAD was soaked in 10^{-2} M tris buffer for 1 min in order to rinse the Nafion for providing a better effect of preconcentration, and then placed on a tissue (KIMTECH Kimwipes) and left to dry at room temperature for about 5 min.

10^{-2} M tris (tris(hydroxymethyl) Aminomethane EQP-ACS) buffer was used as the background electrolyte in all the experiments. The ICP-induced sample preconcentration effect was visualized using fluorescein (fluorescein disodium salt dehydrate, 98+%, Alfa Aesar, USA) as the tracing dye. Finally, the practical feasibility of the proposed μPAD was evaluated using FITC-BSA (Sigma-Aldrich, USA).

B. Experimental setup

Fig. 1 presents a schematic illustration of the proposed paper-based chip. Fig. 1(a) shows the geometry of the μPAD. The channel contains cellulose fibers and a coated nanoporous

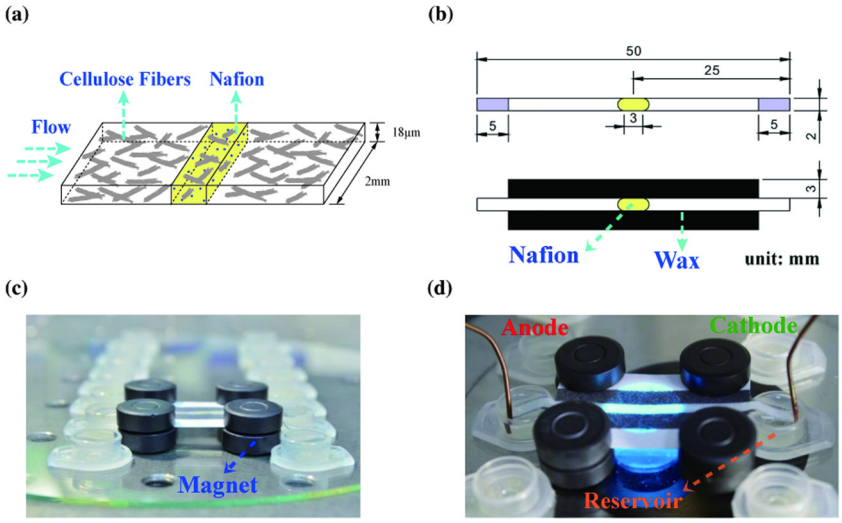

FIG. 1. (a) The μPAD contains cellulose fibers and with a perm-selective Nafion membrane coated at the center of the hydrophilic channel. (b) Schematic illustration of μPAD with straight channel and corresponding dimensions. (c) Side view of μPAD clamped between eight magnets in order to maintain the device in horizontal plane. (d) Photograph showing the device placed on an optical microscope stage for visualization purposes. Copper wires and sample tube lids used as electrodes and reservoirs, respectively.

Nafion membranes penetrating through the thickness (18 μm) of the paper. Fluid is allowed to flow through the channel by capillary/electrokinetic effects. As shown in Fig. 1(b), the μPAD had a total length of 50 mm, but a working length of just 40 mm since the reservoirs at either end of the device have a height of approximately 5 mm. To prevent sagging of the device under the effects of gravity once wetted, the chip was clamped firmly in place between eight magnets placed at its four corners. Notably, this suspended arrangement of the device prevents the working region of the chip from contacting any external solid surface (such as glass), and therefore isolates the electrokinetic forces within the chip from the physical surroundings. The reservoirs were simply realized using the lids of commercial sample tubes due to their small physical volume and the proximity of their height to that of the μPAD when clamped between the magnets (see Figs. 1(c) and 1(d)). Finally, the electrodes at the anode and cathode sides of the device were implemented using simple copper wires with a diameter of 1 mm.

In evaluating the sample concentration performance of the proposed μPADs, the fluorescence signal was observed using an optical microscope (Nikon Eclipse Ti-E, Japan) equipped with a mercury lamp. The images observed through the microscope were captured using a CCD camera (DBK 41BU02, The Imaging Source, Germany) fitted with IC Capture (V.2) software. The external electric field required to induce the ICP effect was provided by a commercial power supply (EC1000S, NF Corporation, Japan). The current-voltage response of the μPADs was measured using a source meter (Model 2400, Keithley Instruments, USA) and exported using LabTracer 2.0 software (Keithley Instruments, USA). Finally, the fluorescence intensity was measured using commercial Image-Pro® Plus software (ImagePro Plus 6.2, Media Cybernetics, USA).

III. RESULTS AND DISCUSSION

In accordance with basic electrokinetics principles, when an electric field is applied to a system comprising an electrolyte and charged channel surfaces, electroosmosis (EOF) and electrophoresis (EP) phenomena spontaneously occur. Leung *et al.*[25] measured the streaming potential of paper (Whatman No. 1 chromatography paper), indicating that the cellulose surface has a non-zero zeta potential. This result implies that the EOF would take place on the μPADs under the application of electric potential. In μPADs, capillary forces play an inevitable effect in inducing sample flow through the channel. Thus, in examining the EOF and EP effects in

the present study, the μPAD was fully wetted before applying the electric field in order to minimize the capillary effect. Moreover, as described above, a perm-selective Nafion membrane was coated on the central region of the hydrophilic paper channel in order to induce the ICP phenomenon. Fig. 2 shows the basic working principle of the proposed μPAD system.

Fig. 3 presents scanning electron microscope (SEM) images of the paper channel with and without the Nafion coating. It is seen in Fig. 3(b) that the Nafion penetrates and fills most of the pores in the paper following the curing process. However, the Nafion contains nanopores, which become ion-selective under the effects of an external electric field. Consequently, as illustrated in Fig. 2, an ICP phenomenon is induced at the interface between the hydrophilic paper channel and the Nafion membrane.

In the present study, the occurrence of the ICP was demonstrated by measuring the current-voltage (I-V) response of a μPAD incorporating a convergent channel. The corresponding results are shown in Fig. 4, and the inset of Fig. 4 illustrates the detailed geometry of the μPAD. As shown, the I-V curve comprises three characteristic regions. In region I, known as the Ohmic region, the current and voltage exhibit a linear relationship, indicating that the conductance of the system remains constant. In region II, referred to as the limiting current region, the current remains approximately constant as the voltage increases. In other words, the conductance decreases, indicating the formation of a depletion zone (see Fig. 2). It is seen that for the considered device, the limiting current is equal to approximately 2.2 μA. In region III, defined as the overlimiting current region, the current-voltage curve for traditional PDMS/glass devices exhibits a nonlinear response due to the depletion zone. For example, vortices are formed due to electroconvection within the depletion zone near the perm-selective interface. Consequently, the conductance increases with an increasing voltage.[31–37] However, for the present device, the current-voltage response in region III does not conform to this typical behavior. Paper is formed of many cellulose fibers and the resulting complicated and intricate structure tends to decrease the electro-convective effect due to significant hydrodynamic resistance to the formation of such vortices. Therefore, in region III of the I-V response curve for the μPAD, the overlimiting current increases only very slightly as the voltage increases. However, it is noted that, as for traditional devices, the curve is nonlinear in the depletion zone. Overall, the results

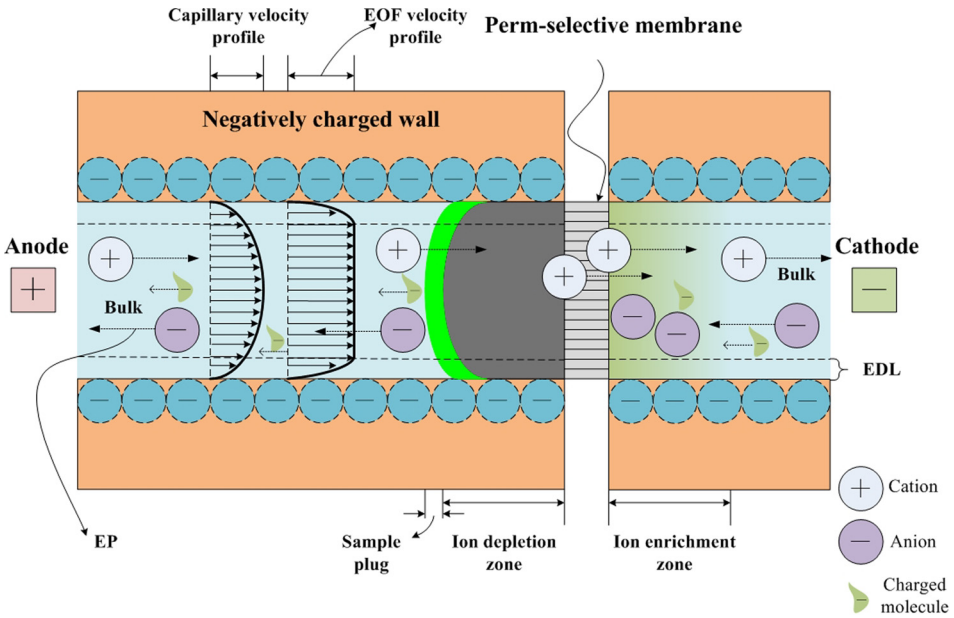

FIG. 2. Schematic illustration shows fluid motion within μPAD channel under application of external electric potential. Cations and anions move toward cathode and anode, respectively, due to electrical migration. Nafion is used as the perm-selective membrane that allows only counter-ions to pass through. Consequently, ICP occurs in which negatively charged molecules accumulate at the upstream side of the membrane resulting in sample concentration effect.

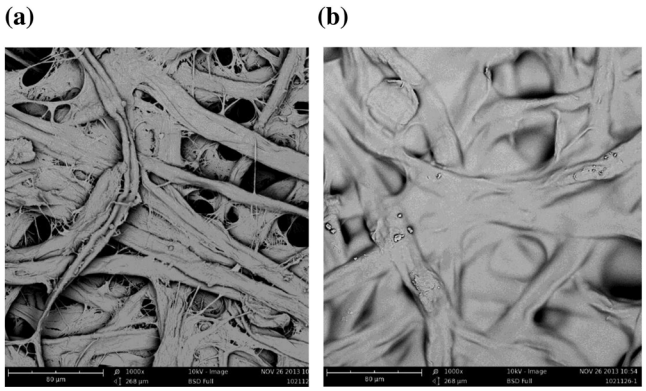

FIG. 3. SEM images of (a) paper and (b) Nafion-coated paper. Black holes in (a) are pores between cellulose fibers. Following the curing process, holes are filled by Nafion as shown in (b).

presented in Fig. 4 show that while the I-V response in the overlimiting region differs from that of a traditional device, the response in the Ohmic and limiting regions is consistent with that reported in the literature. In other words, the results confirm that ICP is induced in a μPAD when the system current reaches the limiting current value.

For a μPAD with a straight channel, the ion transportation is governed mainly by the conductance of the channel. However, for a μPAD with a convergent channel, the ion transport is determined not only by the channel conductance but also by the nozzle-like squeeze effect induced by the variable channel geometry. Fig. 5(a) shows the dimensions of the straight- and convergent-channel μPADs fabricated in the current study. Fig. 5(b) shows the corresponding results obtained for the variation of the conductance with the convergent width in the absence of a Nafion membrane. It is seen that the conductance decreases with a reducing convergent width. Fig. 6 presents schematic illustrations of the considered μPADs with a Nafion membrane and shows the fluorescent images captured of each channel in the maximum sample concentration condition. Fig. 7 shows the variation of the fluorescence intensity and concentration over time in both the straight-channel μPADs (with and without the Nafion membrane) and the

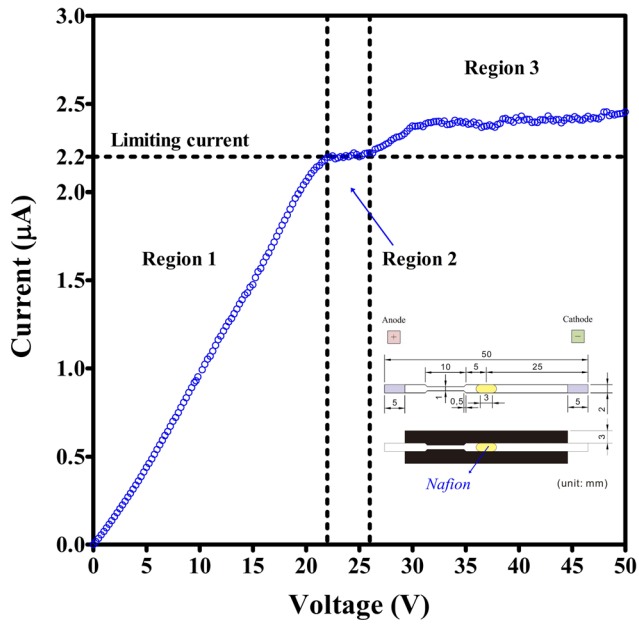

FIG. 4. Current-voltage curve of convergent μPAD with convergent-channel width of 1 mm and 10^{-2} M tris buffer. Three regions are distinguished. Depletion zone formed when voltage reaches approximately 22 V and the ICP is triggered.

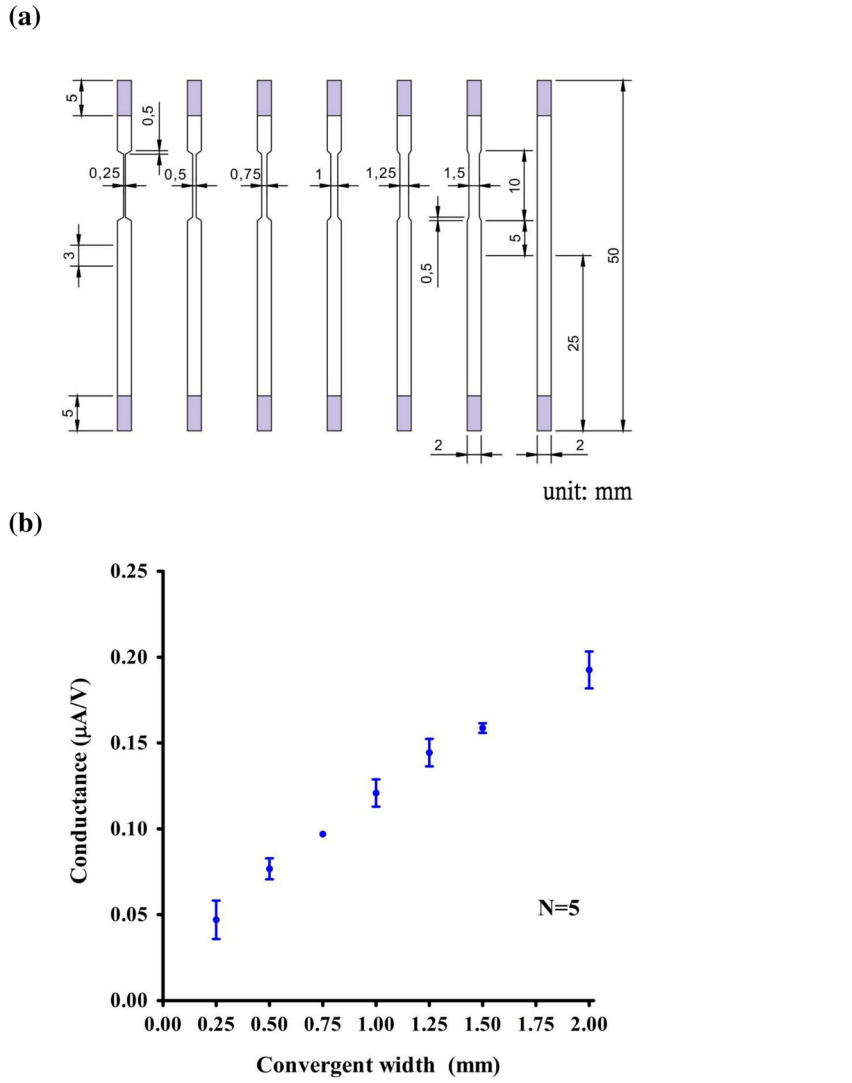

FIG. 5. (a) Schematic illustrations of straight- and convergent-channel μPADs. Left and right 5 mm would be placed into the reservoirs. (b) Variation of conductance with channel width. Note that results correspond to the case where a Nafion membrane is not applied. It shows that the conductance is proportional to the convergent width.

convergent-channel μPADs (with a Nafion membrane). Note that the applied external potential is equal to 50 V in every case. In general, the results presented in Fig. 7 show that the sample concentration performance of the convergent-channel μPADs is superior to that of the straight-channel μPAD in most cases. In other words, the results are consistent with those obtained for a conventional PDMS/glass device.[29] It can be expected that for the fixed amount of concentration will be dispersed more widely in larger space and the concentration will be more closely confined in smaller space. As a result, a better concentration enhancement is found in convergent-channel configurations. In addition, it is seen that a trade-off exists between the effects of a narrower convergent width in enhancing the sample concentration through a nozzle-like squeeze effect and a larger convergent width in enhancing the sample concentration though an increased conductance. Examining the results, it is seen that a convergent width of 1 mm yields the optimal compromise between the two competing effects. Fig. 8 shows the fluorescence intensity in the depletion zone of the corresponding μPAD after 60 s and 130 s, respectively. The animation video can be viewed in the Multimedia view.

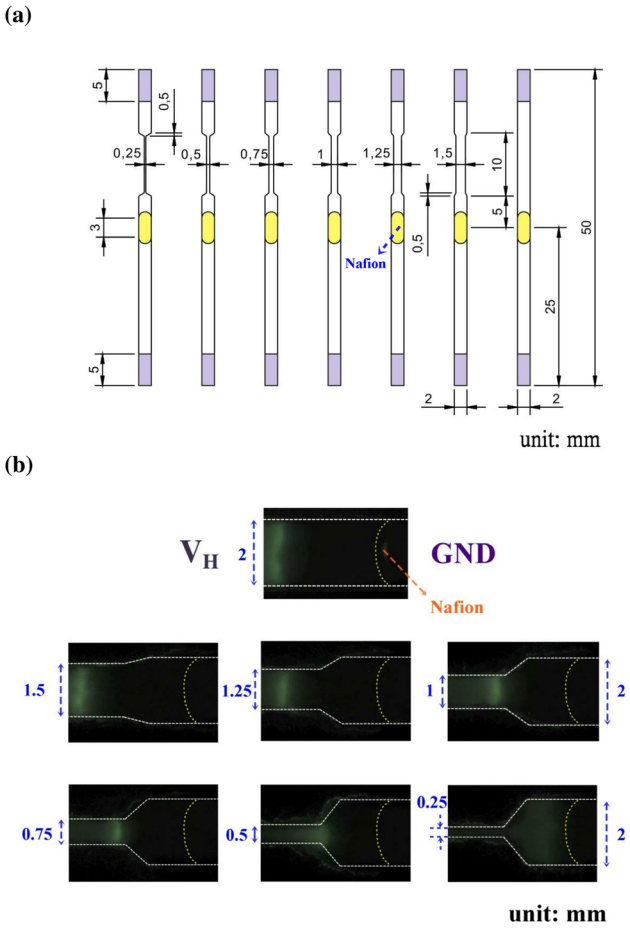

FIG. 6. (a) Schematic illustrations of straight- and convergent-channel μPADs with a Nafion membrane. Nafion is coated at the center of μPAD. (b) Fluorescence images captured at the moment of maximum intensity in straight- and convergent-channel μPADs.

An inspection of Fig. 7 shows that the optimal μPAD device (i.e., a convergent channel width of 1 mm) yields a maximum fluorescein concentration of approximately 20×10^{-5} M. (Note that the initial fluorescein concentration is equal to 10^{-5} M.) Moreover, the time required to reach the maximum concentration condition is equal to approximately 130 s. It is noted that the maximum concentration obtained in the optimized convergent-channel device is around twice that obtained in the straight-channel device with a width of 2 mm (i.e., 10×10^{-5} M after approximately 180 s). Moreover, at the moment when the maximum concentration in the convergent-channel design is obtained (i.e., 130 s), the maximum concentration in the optimized design is approximately three times higher than that obtained in the straight channel.

In traditional PDMS/glass microchannels with a continuous DC bias, the ICP-induced maximum concentration reduces over time as a result of a dispersion effect induced by nonlinear and often unreproducible phenomena associated with a change in the electrical resistance and possibly also the pH.[31] In the present study, this dispersion problem is exacerbated by the fact that the μPAD is directly exposed to the atmosphere and is thus liable to natural evaporation effects. Notably, the evaporation effect is enhanced by the Joule heating induced by the external electric field. Moreover, due to the relatively large potential (50 V), the depletion zone expands over time, causing the associated nonlinear and unpredictable phenomena to become increasingly pronounced.

In the present study, this problem is addressed by means of an adaptive potential control strategy, in which the potential is first set to 50 V for 130 s in order to achieve the maximum

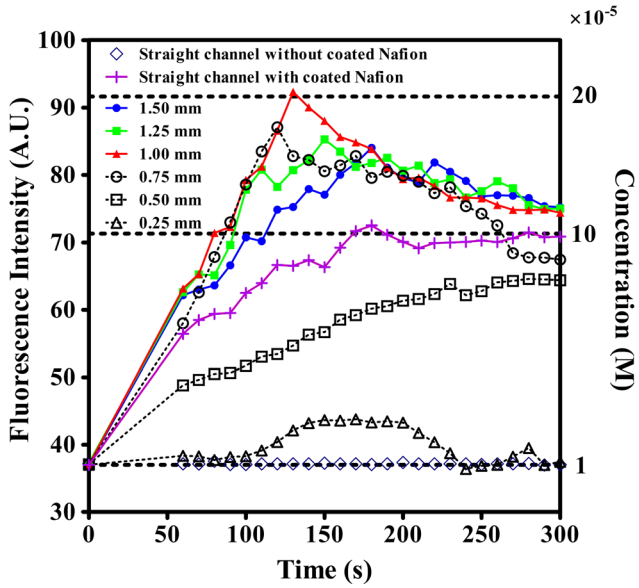

FIG. 7. Variation of fluorescence intensity and sample concentration over time in straight- and convergent-channel μPADs. Note that initial fluorescein concentration is 10^{-5} M and external potential is 50 V. Convergent-width of 1.5 mm yields maximum conductance, but minimum sample squeezing effect. Maximum sample concentration obtained using convergent width of 1.0 mm. Convergent width of 1.0 mm achieves more rapid concentration effect than widths of 1.5 mm or 1.25 mm due to greater squeezing effect. Conversely, narrower convergent widths of 0.5 mm and 0.25 mm achieve poorer concentration effect due to reduced channel conductance.

sample concentration, and is then reduced to 25 V for the remainder of the concentration period. Note that a value of 25 V is specifically chosen here since, as shown in Fig. 4, this value locates within the limiting current region in which the ICP occurs for the optimal convergent-channel design. The results presented in Fig. 9 show that the application of the adaptive voltage control strategy enables the maximum sample concentration condition to be maintained for approximately 20 s. The lowering of the potential after the point of maximum concentration has been achieved is also beneficial in reducing the power consumption (i.e., cost) of the concentration process and minimizing the Joule heating effect. Finally, the adaptive control strategy enables the sample plug to be maintained in an approximately constant position once the point of maximum concentration has been achieved, thereby providing advantages for further applications. The animation video can be viewed in the Multimedia view.

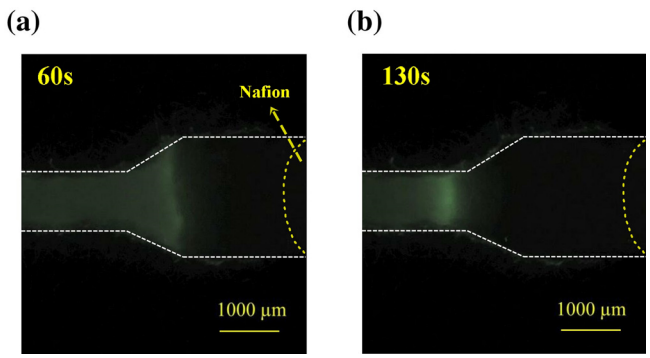

FIG. 8. Fluorescence images captured in optimal convergent-channel μPAD (a) 60 s and (b) 130 s after applying external potential of 50 V. The images show the enhancement of concentration by the geometric effect. Note that initial fluorescein concentration is equal to 10^{-5} M and a convergent channel converging from 2 mm to 1 mm were used. (Multimedia view) [URL: http://dx.doi.org/10.1063/1.4913366.1]

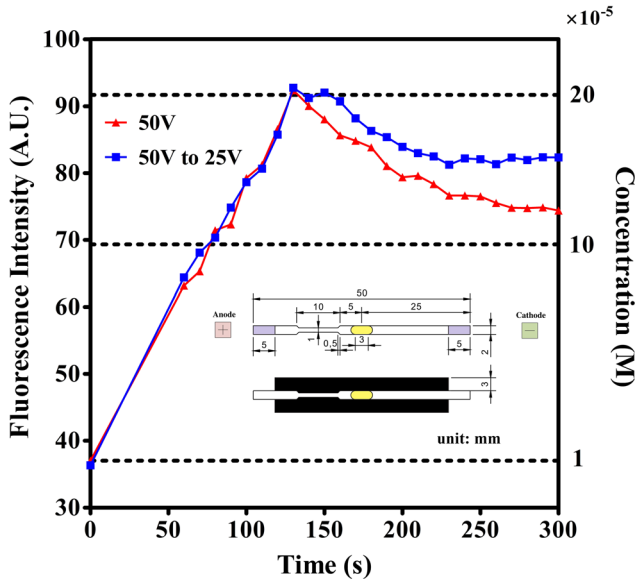

FIG. 9. Variation of fluorescence intensity and sample concentration over time in optimal convergent-channel μPAD given constant potential of 50 V for 300 s or potential of 50 V for 130 s (point of maximum concentration) and reduced potential of 25 V for the remainder of the concentration period. 10^{-5} M fluorescein solution and 10^{-2} M tris buffer were used. (Multimedia view) [URL: http://dx.doi.org/10.1063/1.4913366.2]

The practical feasibility of the proposed optimal convergent-channel μPAD was evaluated by performing the preconcentration of FITC-BSA. Fig. 10 shows the variation of the sample concentration over time given the use of a fixed-potential and variable-potential control strategy, respectively. For the case of a constant potential of 50 V, the FITC-BSA concentration increases by a factor of approximately 15 times within 120 s. (Note that the initial FITC-BSA

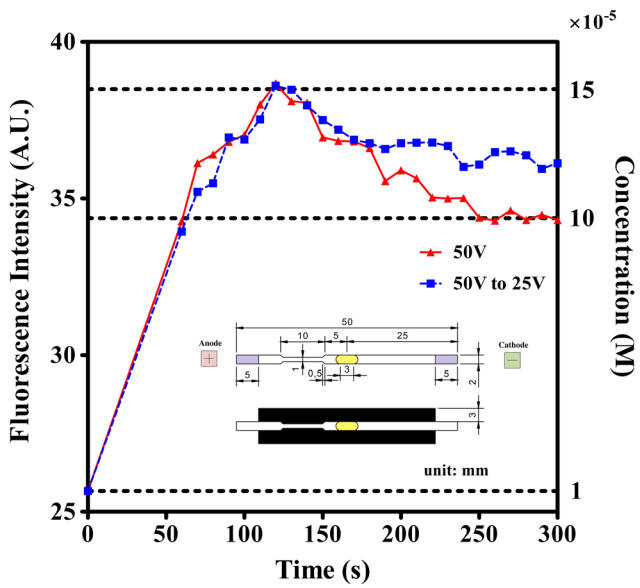

FIG. 10. Sample concentration of FITC-BSA on optimal convergent-channel μPAD with convergent width of 1 mm using either constant potential of 50 V for 300 s or adaptive potential control strategy in which potential is reduced to 25 V after point of maximum concentration. For both strategies, 15-fold improvement in sample concentration is obtained within 120 s. Note that initial FITC-BSA concentration is 10^{-5} M in 10^{-2} M tris buffer. Also, the improved case is also applying 50 V initially but turning down the power from 50 V to 25 V as it reaches 120 s. However, for adaptive potential control strategy, maximum sample concentration condition is maintained for approximately 10 s.

concentration is equal to 10^{-5} M.) However, the sample concentration rapidly reduces following the point of maximum concentration due to dispersion effects. By contrast, given the use of the variable-potential control strategy, the sample concentration remains at a virtually unchanged level for an additional 10 s.

IV. CONCLUSION

This study has performed an experimental investigation into the sample preconcentration on a μPAD patterned with a Nafion membrane. We are the first to measure the current-voltage curve on a Nafion-coated μPAD in order to indicate that the ion depletion occurs and the ion concentration polarization (ICP) is triggered when the current reaches the limiting current. Experiments have been performed to investigate the sample concentration effect in μPADs incorporating either a straight channel with a width of 2 mm or convergent channels with convergent-section widths ranging from 0.25 to 1.5 mm. It has been shown that for a convergent-channel design, a tradeoff exists between the effects of a reducing channel width in enhancing the concentration as a result of a greater nozzle-like squeezing effect on the one hand, and lower channel conductance on the other. The experimental results have revealed that a convergent-channel width of 1 mm represents the optimal value in the present case. Given this optimal channel design, a 20-fold improvement in the initial fluorescein concentration of 10^{-5} M is obtained after 130 s. By contrast, the straight-channel design results in a maximum concentration improvement of just 10 times (after 180 s). In other words, the maximum concentration improvement obtained in the optimized convergent-channel design is around twice that achieved in the straight-channel design. Moreover, after 130 s, the sample concentration achieved using the optimal convergent-channel μPAD is approximately three times higher than that achieved in the straight-channel μPAD after an equivalent time.

As in conventional PDMS/glass-based devices, a significant dispersion effect has been observed in the present μPADs following the point of maximum sample concentration. Previous studies have attributed this phenomenon to nonlinear and often unreproducible effects in the depletion zone. However, it has been speculated that in the present μPADs, the dispersion effect is further enhanced by Joule heating-induced evaporation. Accordingly, an adaptive potential control strategy has been proposed in which the potential is reduced from 50 V to 25 V once the point of maximum sample concentration has been achieved. Note that the 25 V represents the voltage at which the limiting current region exists in the optimal convergent-channel μPAD design. The experimental results have shown that the proposed strategy enables the maximum sample concentration condition to be maintained for around 20 s given a fluorescein sample with an initial concentration of 10^{-5} M. The practicality of the proposed optimal convergent-channel μPAD design has been evaluated using FITC-BSA with an initial concentration of 10^{-5} M. It has been shown that a 15-fold improvement in the sample concentration can be obtained within 120 s given an external voltage of 50 V. Furthermore, by applying the adaptive voltage control strategy, the maximum sample concentration condition can be maintained for approximately 10 s.

ACKNOWLEDGMENTS

The authors gratefully acknowledge the financial support provided to this study by the Ministry of Science and Technology (MOST) of Taiwan under Project Nos. 102-2221-E-006-104-MY3 and 103-2221-E-006-093-MY3.

[1]G. M. Whitesides, Nature **442**, 368–373 (2006).
[2]A. Tefferi and J. Vardiman, Leukemia **22**, 14–22 (2008).
[3]C. D. Chin, V. Linder, and S. K. Sia, Lab Chip **12**, 2118–2134 (2012).
[4]P. Yager, T. Edwards, E. Fu, K. Helton, K. Nelson, M. R. Tam, and B. H. Weigl, Nature **442**, 412–418 (2006).
[5]A. W. Martinez, S. T. Phillips, M. J. Butte, and G. M. Whitesides, Angew. Chem. Int. Ed. **46**, 1318–1320 (2007).
[6]C. H. Weng, M. Y. Chen, C. H. Shen, and R. J. Yang, Biomicrofluidics **8**, 066502 (2014).
[7]I. N. Katis, J. A. Holloway, J. Madsen, S. N. Faust, S. D. Garbis, P. J. S. Smith, D. Voegeli, D. L. Bader, R. W. Eason, and C. L. Sones, Biomicrofluidics **8**, 036502 (2014).
[8]X. Li, D. R. Ballerini, and W. Shen, Biomicrofluidics **6**, 011301 (2012).

[9]A. K. Yetisen, M. S. Akram, and C. R. Lowe, Lab Chip **13**, 2210–2251 (2013).
[10]Y. Song, Y. Y. Huang, X. Liu, X. Zhang, M. Ferrari, and L. Qin, Trends Biotechnol. **32**(3), 132–139 (2014).
[11]M. K. H. G. Setty and I. K. Hewlett, AIDS Res. Treat. **2014**, 497046.
[12]K. Hsieh, A. S. Patterson, B. S. Ferguson, K. W. Plaxco, and H. T. Soh, Angew. Chem. Int. Ed. **51**, 4896–4900 (2012).
[13]S. J. Lo, S. C. Yang, D. J. Yao, J. H. Chen, W. C. Tu, and C. M. Cheng, Lab Chip **13**, 2686–2692 (2013).
[14]C. K. Hsu, H. Y. Huang, W. R. Chen, W. Nishie, H. Ujiie, K. Natsuga, S. T. Fan, H. K. Wang, J. Y. Y. Lee, W. L. Tsai, H. Shimizu, and C. M. Cheng, Anal. Chem. **86**, 4605–4610 (2014).
[15]R. Y. T. Chiu, E. Jue, A. T. Yip, A. R. Berg, S. J. Wang, A. R. Kivnick, P. T. Nguyen, and D. T. Kamei, Lab Chip **14**, 3021–3028 (2014).
[16]M. C. Morales, H. Lin, and J. D. Zahn, Lab Chip **12**, 99–108 (2012).
[17]C. C. Lin, J. L. Hsu, and G. B. Lee, Microfluid. Nanofluid. **10**, 481–511 (2011).
[18]K. D. Huang and R. J. Yang, Electrophoresis **29**, 4862–4870 (2008).
[19]A. K. Singh, D. J. Throckmorton, B. J. Kirby, and A. P. Thompson, *Micro Total Analysis Systems* (Kluwer Academic Publishers, 2002), Vol. I, pp. 347–349.
[20]R. S. Foote, J. Khandurina, S. C. Jacobson, and J. M. Ramsey, Anal. Chem. **77**, 57–63 (2005).
[21]S. M. Kim, M. A. Burns, and E. F. Hasselbrink, Anal. Chem. **78**, 4779–4785 (2006).
[22]S. J. Kim, Y. A. Song, and J. Han, Chem. Soc. Rev. **39**(3), 912–922 (2010).
[23]M. Kim, M. Jia, and T. Kim, Analyst **138**, 1370–1378 (2013).
[24]E. Fu, T. Liang, P. S. Mihalic, J. Houghtaling, S. Ramachandran, and P. Yager, Anal. Chem. **84**, 4574–4579 (2012).
[25]V. Leung, A. A. M. Shehata, C. D. M. Filipe, and R. Pelton, Colloids Surf., A **364**, 16–18 (2010).
[26]M. M. Gong, P. Zhang, B. D. MacDonald, and D. Sinton, Anal. Chem. **86**, 8090–8097 (2014).
[27]R. Ibanez, D. F. Stamatialis, and M. Wesslin, J. Membr. Sci. **239**, 119–128 (2004).
[28]J. J. Krol, M. Wessling, and H. Strathmann, J. Membr. Sci. **162**, 145–154 (1999).
[29]C. L. Chen and R. J. Yang, Electrophoresis **33**, 751–757 (2012).
[30]E. Carrilho, A. W. Martinez, and G. M. Whitesides, Anal. Chem. **81**, 7091–7095 (2009).
[31]A. Höltzel and U. Tallarek, J. Sep. Sci. **30**, 1398–1419 (2007).
[32]I. Rubinstein and B. Zaltzman, Phys. Rev. E **62**(2), 2238–2251 (2000).
[33]S. J. Kim, Y. C. Wang, J. H. Lee, H. Jang, and J. Han, Phys. Rev. Lett. **99**, 044501 (2007).
[34]K. D. Huang and R. J. Yang, Microfluid. Nanofluid. **5**, 631–638 (2008).
[35]G. Yossifon and H. C. Chang, Phys. Rev. Lett. **101**, 254501 (2008).
[36]H. C. Chang, G. Yossifon, and E. A. Demekhin, Annu. Rev. Fluid Mech. **44**, 401–426 (2012).
[37]Z. Slouka, S. Senapati, and H. C. Chang, Annu. Rev. Anal. Chem. **7**, 317–335 (2014).